

## RESEARCH ARTICLE

View Article Online

View Journal | View Issue

Cite this: *Org. Chem. Front.*, 2025, 12, 3230Pd-catalyzed site-specific heteroaromatic C–H/*peri*-C–H annulative coupling for synthesis of cyclopenta-fused polycyclic heteroarenes†Tienan Jin, \*<sup>b</sup> Masaki Kawata,<sup>a</sup> Sho Aida<sup>a</sup> and Masahiro Terada <sup>a</sup>

Cyclopenta-fused polycyclic heteroarenes (CP-PHAs) composed of acenaphthylene and heteroaromatic units have emerged as intriguing photoelectronic materials in view of the electron-accepting feature of the fused CP rings and the tunable electronic properties of the heteroareomatics. To date, Pd-catalyzed aromatic C–H/*peri*-C–halogen coupling has been used as one of the most general methods to construct such CP-rings. In contrast, Pd-catalyzed direct aromatic C–H/*peri*-C–H coupling may provide a shortcut to this CP-ring formation, which is applicable to a wide range of polycyclic arenes bearing *peri*-C–H bonds, but remains unexploited so far. We herein describe a Pd-catalyzed site-specific C–H/*peri*-C–H annulative coupling between (benzo)thiophenes or indoles with various polycyclic arenes to access a variety of  $\pi$ -extended CP-PHAs. Benzo[*b*]thiophenes or thiophenes with a 1-naphthalenyl group at the C3 position gave C2-naphthylated CP-PHAs in the Pd(OPiv)<sub>2</sub>/AgOPiv system, whereas indoles with a 1-naphthalenyl group at the C2 position gave C3-naphthylated CP-PHAs in the Pd(OPiv)<sub>2</sub>/AgSbF<sub>6</sub> system. Notably, deuteration experiments demonstrated that silver salts play a crucial role in the formation of heteroaryl–Ag species *via* site-specific C–H metalation of heteroareomatics, which subsequently undergo transmetalation with Pd(II) to form heteroaryl–Pd species and activate the *peri*-C–H bond of the naphthalene group. Furthermore, this method enables the synthesis of structurally diverse CP-PHAs *via* activation of *peri*-C–H bonds in large polycyclic aromatic hydrocarbons such as anthracene, phenanthrene, and pyrene.

Received 7th January 2025,

Accepted 4th March 2025

DOI: 10.1039/d5qo00034c

rsc.li/frontiers-organic

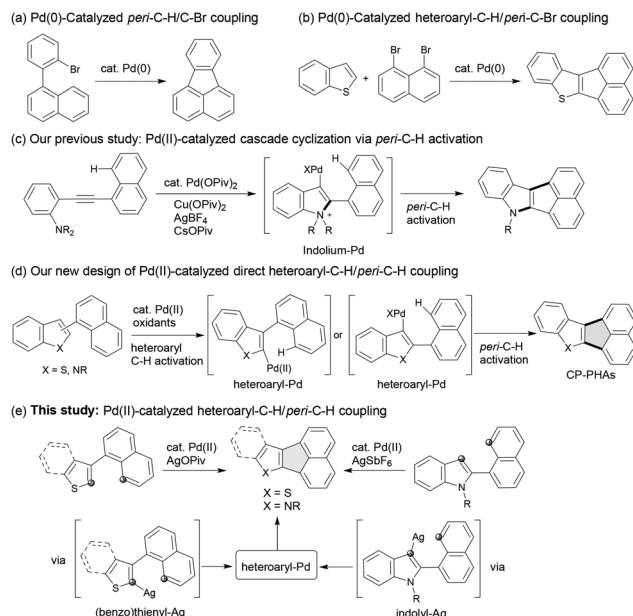
## Introduction

Cyclopenta-fused polycyclic aromatic hydrocarbons (CP-PAHs) and polycyclic heteroareomatics (CP-PHAs) have emerged as intriguing photoelectronic materials in terms of unique electronic affinity of the fused CP rings and their enhanced stability.<sup>1–5</sup> Among them, CP-PHAs composed of acenaphthylene and heteroareomatic units have drawn particular interest due to the electron-accepting nature of acenaphthylene and the tunable electronic properties of the heteroareomatics.<sup>4,5</sup> In this context, we are interested in developing new and highly efficient synthetic methods to construct  $\pi$ -extended CP-PHAs fused with electron-rich heteroareomatic and electron-accepting acenaphthylene units to create a new class of donor–acceptor (D–A) type  $\pi$ -electronic molecules. To date, the Pd(0)-catalyzed aromatic *peri*-C–H/C–Br and heteroareomatic C–H/*peri*-C–Br annulative couplings are the most efficient methods toward

constructing such acenaphthylene-fused CP-PAHs and CP-PHAs (Scheme 1a and b).<sup>6–8</sup> However, these methods require brominated arenes, and the extension to other  $\pi$ -extended PAHs with *peri*-positions is considered problematic, particularly the method using 1,8-dibromonaphthalene (Scheme 1b), due to the difficult in selective prefunctionalization of the *peri*-positions of such PAHs. Recently, we also developed a novel Pd(II)-catalyzed cascade cyclization *via* *peri*-C–H activation for the construction of indole- and acenaphthylene-fused D–A type CP-PHAs (Scheme 1c),<sup>9</sup> but this method was limited to the formation of the indole moiety. Considering that this cascade cyclization leads to the formation of an indolyl–Pd intermediate<sup>9,10</sup> enabling subsequent *peri*-C–H bond activation, we envisioned that if heteroaryl–Pd intermediates can be formed site-selectively from readily available naphthyl-substituted benzo[*b*]thiophene, thiophene, and indole substrates, the desired CP-PHAs fused with naphthalene can be constructed conveniently by direct C–H/*peri*-C–H annulative coupling (Scheme 1d).<sup>6,9,11</sup>

Transition-metal-catalyzed oxidative aromatic C–H/C–H coupling reactions, which do not require prefunctionalization of (hetero)aromatic substrates, have been demonstrated to be a promising strategy for the synthesis of biaryl and polycyclic (hetero)aromatic motifs,<sup>12</sup> structural fragments frequently

<sup>a</sup>Department of Chemistry, Graduate School of Science, Tohoku University, Sendai 980-8578, Japan<sup>b</sup>Research and Analytical Center for Giant Molecules, Graduate School of Science, Tohoku University, Sendai 980-8578, Japan. E-mail: tetsuo.kin.a6@tohoku.ac.jp† Electronic supplementary information (ESI) available. See DOI: <https://doi.org/10.1039/d5qo00034c>



**Scheme 1** Pd-catalyzed synthesis of fused acenaphthylenes via (hetero)aromatic C-H bond activation.

used in optoelectronic materials and medicinal chemistry. In particular, depending on the inherent differences in reactivity at the C2 and C3 positions and the catalyst system, a variety of site-selective C-H arylations of (benzo)thiophenes and indoles have been reported to afford biaryls.<sup>13–15</sup> However, aromatic C-H/*peri*-C-H coupling of (benzo)thiophenes or indoles with naphthalenes provides a shortcut to CP ring formation by intramolecular direct coupling, which may be applicable to a wide range of polycyclic arenes bearing *peri*-C-H bonds, but remains unexplored so far. We herein describe a Pd-catalyzed site-specific heteroaromatic C-H/*peri*-C-H annulative coupling between (benzo)thiophenes or indoles and various PAHs bearing C-H bonds to access structurally diverse  $\pi$ -extended CP-PHAs (Scheme 1e). Furthermore, we have demonstrated that silver salt additives with different counteranions function not only as oxidants but also as site-specific C-H metalation reagents to form heteroaryl-Ag intermediates followed by Pd(II)-catalyzed transmetalation to generate the desired heteroaryl-Pd intermediates.

## Results and discussion

Taking into account the influence in acidity of the C-H bonds at the C2 ( $pK_a = 32.0$ ) and C3 ( $pK_a = 36.8$ ) positions of benzo[*b*]thiophene on the dehydrometalation reactivity,<sup>16</sup> 2-(naphthalen-1-yl)benzo[*b*]thiophene **1a** was selected as the substrate to optimize the reaction conditions for the synthesis of benzo[*b*]thiophene-fused CP-PHA **2a**. As shown in Scheme 1c,<sup>9</sup> we previously reported that the Pd(OPiv)<sub>2</sub> catalyst favors the activation of *peri*-C-H bonds of PAHs and an additional metal oxidant is required to regenerate active Pd(II) species from the *in situ* formed Pd(0) species. With these con-

siderations in mind, we evaluated a set of Pd(II) (10 mol%) catalysts and metal oxidants (3 equiv.) by using *N,N*-dimethyl acetamide (DMAc) as the solvent at 120 °C for 14 h (Table 1). As expected, the use of the Pd(OPiv)<sub>2</sub> catalyst in the absence of oxidants, **2a** was obtained in a very low yield of 5% (entry 1). The use of cationic silver salts such as AgSbF<sub>6</sub> and AgBF<sub>4</sub> as oxidants had no obvious effect on improving the yield of **2a** (entries 2 and 3). Subsequently, AgOAc oxidant was used to promote the carboxylate-assisted C-H bond metalation, but although a slight increase in efficiency was observed, the yield of **2a** was still low (entry 4). To our delight, the reaction efficiency drastically enhanced when AgOPiv oxidant was used, affording **2a** in 81% yield in 3 h (entry 5). It was mentioned that the use of a reduced amount of AgOPiv (2 equiv.) resulted in a decrease in the yield of **2a** along with the recovered **1a** (entry 6). Moreover, the combination of AgOPiv oxidant with PdCl<sub>2</sub> or Pd(OAc)<sub>2</sub> catalyst instead of Pd(OPiv)<sub>2</sub> also showed sufficient efficiency for the formation of **2a** (entries 7 and 8). However, the use of Cu(OPiv)<sub>2</sub> instead of AgOPiv was ineffective in improving the yield of **2a** (entry 9). These results indicate that the existence of high concentrations of pivalate counter anion in AgOPiv is crucial for the implementation of the present C-H/C-H coupling reaction. In addition, the optimized catalyst system in entry 5 showed higher activity in polar solvents such as DMAc, DMF (71%), NMP (65%), *i*-PrCN (62%), and 1,4-dioxane (70%) than in less polar solvents such as toluene (33%) and chlorobenzene (40%).

To verify the difference in reactivity of the C-H bonds at the C2 and C3 positions, the reaction of 2-(naphthalen-1-yl)benzo[*b*]thiophene **1a'** was performed under the optimized conditions (eqn (1)). As a result, the desired product **2a** was obtained in only 3% yield and **1a'** was mainly recovered, indicating that the reactivity of the C-H bond at the C3 position of

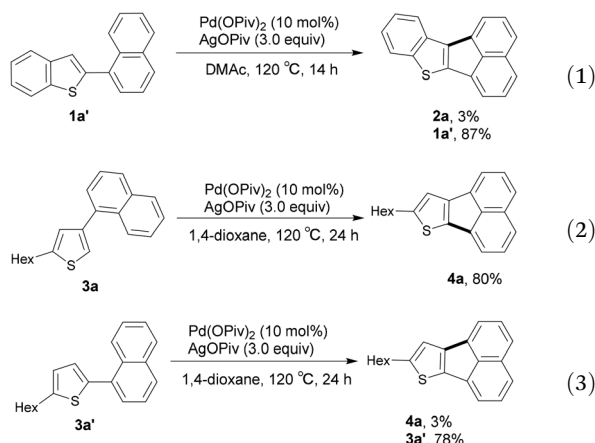
**Table 1** Optimization of reaction conditions for the coupling of 3-(naphthalen-1-yl)benzo[*b*]thiophene (**1a**)<sup>a</sup>

Entry	Pd(II)	Oxidant	<b>2a</b> <sup>b</sup> (%)	<b>1a</b> <sup>b</sup> (%)
1	Pd(OPiv) <sub>2</sub>	None	5	93
2	Pd(OPiv) <sub>2</sub>	AgSbF <sub>6</sub>	10	88
3	Pd(OPiv) <sub>2</sub>	AgBF <sub>4</sub>	12	85
4	Pd(OPiv) <sub>2</sub>	AgOAc	37	46
5 <sup>c</sup>	Pd(OPiv) <sub>2</sub>	AgOPiv	81 (78)	0
6 <sup>d</sup>	Pd(OPiv) <sub>2</sub>	AgOPiv	63	20
7	PdCl <sub>2</sub>	AgOPiv	75	0
8	Pd(OAc) <sub>2</sub>	AgOPiv	74	0
9	Pd(OPiv) <sub>2</sub>	Cu(OPiv) <sub>2</sub>	20	63

<sup>a</sup> Unless otherwise noted, the reaction carried out with **1a** (0.2 mmol), Pd(II) catalyst (0.02 mmol), oxidant (0.6 mmol) in DMAc (2 mL) at 120 °C for 14 h. <sup>b</sup> <sup>1</sup>H NMR yields determined using CH<sub>2</sub>Br<sub>2</sub> as an internal standard. Isolated yield was shown in parentheses. <sup>c</sup> Reaction time is 3 h. <sup>d</sup> 2 equiv. of AgOPiv (0.4 mmol) was used.

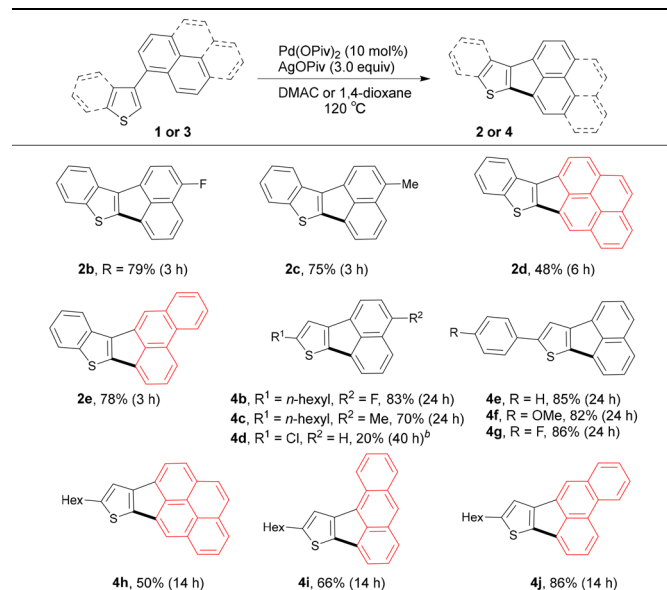


the benzo[*b*]thiophene moiety is much lower than that at the C2 position in this catalyst system. Next, the same catalytic system was used to investigate the site-selectivity of C–H bonds at the C2 and C3 positions of thiophene substrates. It has also been reported that the C–H bond acidity is higher at the C2 ( $pK_a = 33.5$ ) position of thiophene than at the C3 ( $pK_a = 39.0$ ) position.<sup>16</sup> Similar to the site-selectivity of benzo[*b*]thiophene substrates, thiophene substrate **3a** bearing a 1-naphthyl group at the C3 position produced corresponding product **4a** in a high yield of 80% (eqn (2)), whereas thiophene substrate **3a'** bearing a 1-naphthyl group at the C2 position afforded a very poor yield of **4a** (eqn (3)). These results indicate that in the present catalytic system, the C–H bond at the C2 position of the thiophene moiety is much more reactive than the C–H bond at the C3 position.



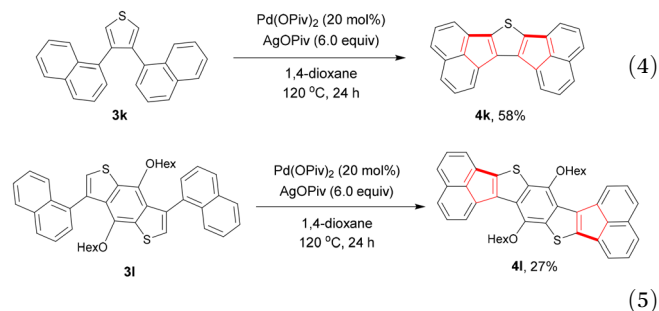
With the site-selective reactivity in hand, the substrate scope of benzo[*b*]thiophenes **1** and thiophenes **3** was evaluated under optimized conditions (Table 2).<sup>17</sup> The electron-withdrawing fluorine group and electron-donating methyl group at the 4-position of the naphthyl moiety in the benzo[*b*]thiophene substrates, respectively, had negligible electronic effect on the dual C–H bond activation process, yielding corresponding CP-PHAs **2b** and **2c** in good yields. Remarkably, the *peri*-C–H bonds in large PAHs such as pyrene and phenanthrene moieties could also be activated to construct  $\pi$ -extended CP-PHAs **2d** and **2e** in 48% and 78% yields, respectively. Likewise, thiophene substrates bearing fluorine and methyl substituents at the 4-position of the 1-naphthyl moiety, respectively, did not show significant electronic effect on the reactivity difference, affording corresponding CP-PHAs **4b** and **4c** in good yields. In comparison, the thiophene substrate **3d**, 2-chloro-4-(naphthalen-1-yl)thiophene, bearing a chlorine substituent at the 2-position of the thiophene ring, exhibited low reactivity under the standard conditions, affording the annulation product **4d** in 20% yield. However, most of the chlorine substituent remained unreacted under the conditions and **3d** was recovered in 65% yield albeit with the formation of a trace of the dechlorinated byproduct of **3d**. Aryl units such as unsubstituted phenyl, and 4-MeO- and 4-F-substituted phenyls on the thiophene moiety did not affect this C–H/C–H coupling, affording desired products **4e–g** in high yields. Gratifyingly,

**Table 2** Synthesis of various  $\pi$ -extended CP-PHAs fused with benzo[*b*]thiophenes and thiophenes<sup>a</sup>



<sup>a</sup> Reaction conditions: benzo[*b*]thiophenes **1** or thiophenes **3** (0.2 mmol), Pd(OPiv)<sub>2</sub> (10 mol%), AgOPiv (3 equiv.), DMAc (0.1 M) for substrates **1** and 1,4-dioxane (0.1 M) for substrates **2**, 120 °C. Isolated yields are shown. <sup>b</sup> The starting substrate **3d** was recovered in 65% yield.

large PAHs such as pyrene, anthracene, and phenanthrene having *peri*-C–H bonds showed good compatibility for the present C–C/H coupling, giving the  $\pi$ -extended CP-PHAs **4h–j** in good to high yields. Furthermore, large CP-PHA structures fused with two strained CP rings could be constructed by the two-fold C–H/*peri*-C–H coupling strategy. For example, the reaction of **3k** bearing two 1-naphthyl groups at the C3- and C4-positions of the thiophene under the modified conditions led to the cleavage of four C–H bonds to give corresponding product **4k** in 58% yield (eqn (4)). Furthermore, with regard to the prospective application of the highly  $\pi$ -extended CP-PHAs as optoelectronic materials,<sup>8</sup> the reaction of **3l** consisting of a benzo[1,2-*b*:4,5-*b'*]dithiophene core and two 1-naphthyl groups was carried out, enabling the two-fold C–H/*peri*-C–H coupling to afford desired product **4l** in 27% yield.

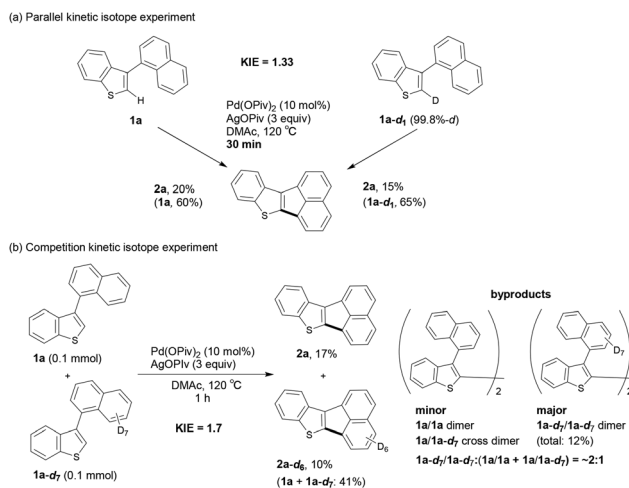


To gain insights into the site-selective metalation process, several deuteration reactions were performed. The reaction of **1a** with D<sub>2</sub>O in the presence of 1 equiv. of Pd(OPiv)<sub>2</sub> without



using AgOPiv afforded the deuterated benzo[*b*]thiophene **1a-d<sub>1</sub>** in 3% yield along with the desired coupling product in 25% yield (Scheme 2a). This result implies that C–H metalation with Pd(II) at the C2 position of **1a** leads to the formation of a **Bt-Pd** intermediate, enabling subsequent *peri*-C–H bond activation, but in much lower yield compared to those using Pd(II) catalyzed conditions in combination with AgOPiv. Sanford and Larrosa demonstrated that silver salts such as AgOPiv and Ag<sub>2</sub>O promoted the C–H metalation of thiophene and benzo[*b*]thiophene at the C2 position to form a **Bt-Ag** intermediate.<sup>14b,18</sup> Based on these precedents and our optimized conditions, the reaction of **1a** with D<sub>2</sub>O was carried out using 1 equiv. of AgOPiv in the absence of Pd(II) catalyst. As a result, deuterated **1a-d<sub>1</sub>** was obtained in 44% yield without forming the coupling product **2a**. This H/D exchange indicates the formation of a **Bt-Ag** intermediate, which should be a key intermediate for the Pd(II)-catalysed transmetalation reaction to produce the **Bt-Pd** intermediate. Additionally, high resolution mass spectrometry (HRMS) analysis confirmed that no deuterium was incorporated at the 2- or 8-positions of the naphthyl moiety in **1a**, **1a-d<sub>1</sub>**, and **2a** after these deuteration reactions. In contrast, no obvious H/D exchange was detected when **1a'** was reacted with D<sub>2</sub>O using AgSbF<sub>6</sub> and AgOPiv, respectively (Scheme 2b), which is in line with the result shown in eqn (1), suggesting that the C–H bond at the C3 position of **1a'** is almost inactive in the present catalyst system.

In addition, parallel kinetic isotope effect (KIE) reactions with protonated **1a** and deuterated **1a-d<sub>1</sub>** were carried out in separated vessels for 30 min under optimized conditions (Scheme 3a). The low KIE value of 1.33 indicates that the C–H bond activation at the C2 position is unlikely to be the rate-determining step. Furthermore, a KIE value of 1.7 was obtained in the intermolecular competition reaction using a 1:1 mixture of **1a** and **1a-d<sub>7</sub>** under optimized conditions in the same vessel for 1 h (Scheme 3b). It should be noted that in the reaction of **1a** under standard conditions (shown in

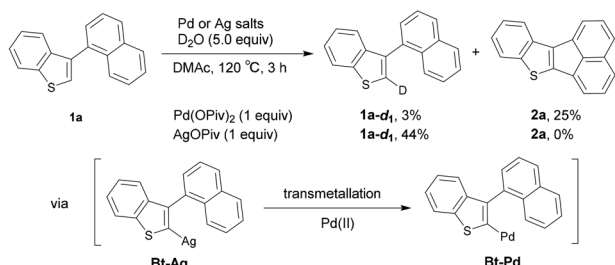


**Scheme 3** Study of deuterium kinetic isotope effect (KIE) for C–H metalation. <sup>1</sup>H NMR yields are shown using CH<sub>2</sub>Br<sub>2</sub> as an internal standard.

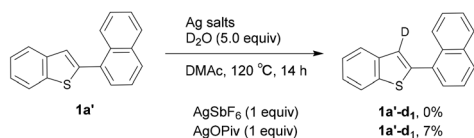
Table 1, entry 5), the dimerization product **1a/1a** was observed as a byproduct in less than 5% yield. This competition KIE reaction afforded a mixture of dimerization byproducts with a total yield of 12%, including the deuterated homo-coupling dimer **1a-d<sub>7</sub>/1a-d<sub>7</sub>** as the major byproduct and the protonated homo-coupling dimer **1a/1a** and cross-coupling dimer **1a/1a-d<sub>7</sub>** as minor byproducts (~2:1 ratio). The formation of **1a-d<sub>7</sub>/1a-d<sub>7</sub>** dimer as the major byproduct and the higher KIE value than the parallel reaction suggest that the *peri*-C–H bond activation may be the rate-determining step.

On the basis of experimental outcomes and the prominent role of the pivalate counteranion in this transformation, a plausible reaction mechanism is outlined in Scheme 4. Both AgOPiv and Pd(OPiv)<sub>2</sub> enable the activation of the C–H bond of **1a** at the C2 position by a pivalate-assisted concerted metalation deprotonation (CMD) process *via* transition state **TS1**.<sup>19</sup> In this case, in terms of the C–H metalation efficiency shown in Scheme 2a, the AgOPiv-mediated C–H metalation should predominantly proceed compared to Pd(OPiv)<sub>2</sub>, affording **Bt-Ag** inter-

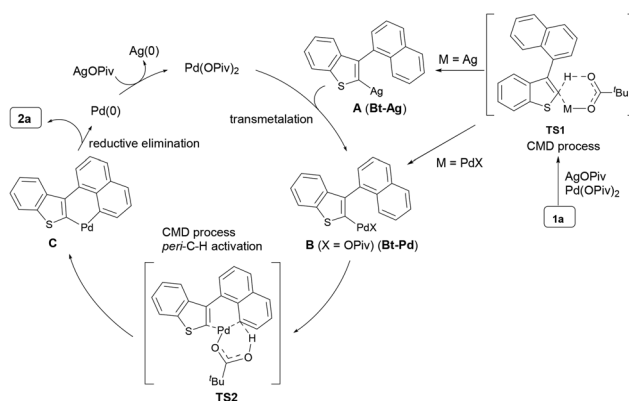
(a) Deuteration of the 2-position of **1a**



(b) Deuteration of the 3-position of **1a'**



**Scheme 2** Study for the role of Ag and Pd salts. <sup>1</sup>H NMR yields are shown using CH<sub>2</sub>Br<sub>2</sub> as an internal standard.



**Scheme 4** Plausible reaction mechanism for the formation of **2a**.



mediate **A** and **Bt-Pd** intermediate **B**, the latter of which also can be formed from the former *via* transmetalation with Pd(OPiv)<sub>2</sub>. The *peri*-C–H bond of intermediate **B** is then activated by an intramolecular CMD process *via* transition state **TS2**, leading to the formation of palladacycle **C**. Reductive elimination of **C** produces the corresponding product **2a** along with Pd(0) species, the latter of which can be oxidized by AgOPiv oxidant to regenerate the active Pd(OPiv)<sub>2</sub> catalyst.

The UV-Vis absorption of representative CP-PHAs in chloroform solution showed broad absorption spectra extending up to about 600 nm (Fig. 1). The longest absorption maxima ( $\lambda_{\text{max}}$ ) and onsets of **2d**, **4h**, and **4i** fused with large  $\pi$ -surfaces of pyrene (**2d** and **4h**) and anthracene (**4i**), respectively, are redshifted compared to **2a** fused with naphthalene due to the large  $\pi$ -extension of the formers (Fig. 1a). Notably, these CP-PHAs with one embedded CP ring exhibit very weak absorbance in the range of 400–600 nm, which can be attributed to the HOMO–LUMO transition with very small oscillator strengths ( $f = 0.0236$ – $0.0074$ ) as suggested by density functional theory (DFT) calculations at the B3LYP/6-31+G(d) level (Fig. S1, ESI†). In comparison, **4k** and **4l** fused with two CP rings show increased absorption intensities with  $\lambda_{\text{max}}$  of 510 nm and 552 nm, respectively, corresponding to the HOMO–LUMO transitions by DFT calculations ( $f = 0.1606$ – $0.1141$ ) (Fig. 1b and Fig. S1†). The absorption onset of 590 nm for **4l** is redshifted compared to **4k** (522 nm) due to the large  $\pi$ -extension system of **4l**. The HOMO and LUMO energy levels of CP-PHAs were calculated from the oxidation and reduction potentials by cyclic voltammetry (Table 3 and Fig. S2 in ESI†). Relatively low-lying HOMO and LUMO were observed in the range of  $-5.59$  to  $-5.37$  eV for **2a**–**4k** and  $-3.61$  to  $-3.48$  eV for **2a**–**4l**, respectively, due to the high electron affinity of the fused CP rings, in agreement with the trend of DFT calculations. **4l** fused with two CP rings has a high HOMO of  $-5.16$  eV due to the strong electron-donating benzo-dithiophene core and two alkoxy groups. The electronic structures studied by DFT calculations suggest that the LUMO contours of **2a**, **2d**, **4h**, and **4i** are mainly localized at the acenaphthylene core and peripheral polyaromatic units, whereas the HOMOs are delocalized from the (benzo)thiophene moiety to the acenaphthylene moiety. In addition, the HOMO and LUMO of **4l** are located at the benzodithiophene core and two

**Table 3** Electrochemical properties of CP-PHAs

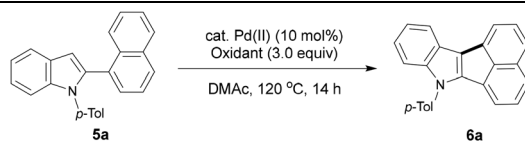
Compd.	$\Delta E^a$ [eV]	HOMO <sup>b</sup> [eV]	HOMO <sup>c</sup> [eV]	LUMO <sup>b</sup> [eV]	LUMO <sup>c</sup> [eV]
<b>2a</b>	2.07	−5.59	−5.38	−3.52	−2.03
<b>2d</b>	2.00	−5.48	−5.22	−3.48	−2.23
<b>4h</b>	1.97	−5.45	−5.22	−3.48	−2.04
<b>4i</b>	1.97	−5.45	−5.18	−3.48	−2.18
<b>4k</b>	1.85	−5.37	−5.17	−3.52	−2.08
<b>4l</b>	1.55	−5.16	−4.81	−3.61	−2.12

<sup>a</sup> HOMO–LUMO energy gap ( $\Delta E$ ) was calculated from the HOMO and LUMO energy levels. <sup>b</sup> HOMO and LUMO was calculated from the oxidation and reduction potentials by CV measurement and the Fc/Fc<sup>+</sup> (−4.80 eV) was used as an external standard. <sup>c</sup> DFT calculation at the B3LYP/6-31+G(d) level.

acenaphthylene cores, respectively, exhibiting a D–A type electronic structure consistent with the high-lying HOMO and low-lying LUMO energy levels.

Next, we continued to develop the site-specific C–H/*peri*-C–H coupling of 1-naphthylene-tethered indoles to construct indole-fused CP-PHAs. The indole bearing an *N*-methyl substituent was investigated to have less acidic C–H bonds at the C2 ( $pK_a = 37.7$ ) and C3 ( $pK_a = 41.4$ ) positions compared to (benzo)thiophenes.<sup>16</sup> Therefore, considering the high nucleophilicity of the C3 position of indoles, the 1-(*p*-tolyl)-1*H*-indole **5a** bearing 1-naphthyl group at the C2 position was selected as the substrate to establish optimal catalyst system. A brief optimization of the conditions showed that the use of the Pd(OPiv)<sub>2</sub> catalyst in the absence of an oxidant was almost ineffective in the formation of the corresponding product **6a** (Table 4, entry 1). Importantly, cationic AgSbF<sub>6</sub> and AgBF<sub>4</sub> proved to be highly effective oxidants in improving the yield of **6a**, whereas the AgOPiv oxidant, which has been successfully used in the case of (benzo)thiophenes, showed moderate reactivity (entries 2–4). This prominent role of cationic silver salts suggests the involvement of an electrophilic metalation

**Table 4** Optimization of reaction conditions for (hetero)aromatic C–H/C–H coupling with indole substrates<sup>a</sup>

				
Entry	Pd(II)	Oxidant	<b>6a</b> <sup>b</sup> (%)	<b>5a</b> <sup>b</sup> (%)
1	Pd(OPiv) <sub>2</sub>	None	6	80
2	Pd(OPiv) <sub>2</sub>	AgSbF <sub>6</sub>	72 (65)	0
3	Pd(OPiv) <sub>2</sub>	AgBF <sub>4</sub>	73	5
4	Pd(OPiv) <sub>2</sub>	AgOPiv	54	19
5	Pd(OPiv) <sub>2</sub>	Cu(OPiv) <sub>2</sub>	36	31
6	Pd(OPiv) <sub>2</sub>	Cu(OTf) <sub>2</sub>	28	51
7	PdCl <sub>2</sub>	AgSbF <sub>6</sub>	14	85

<sup>a</sup> Unless otherwise noted, the reaction carried out with **1a** (0.2 mmol), Pd(II) catalyst (0.02 mmol), oxidant (0.6 mmol) in DMAc (2 mL) at 120 °C for 14 h. <sup>b</sup> <sup>1</sup>H NMR yields determined using CH<sub>2</sub>Br<sub>2</sub> as an internal standard. Isolated yield was shown in parentheses.

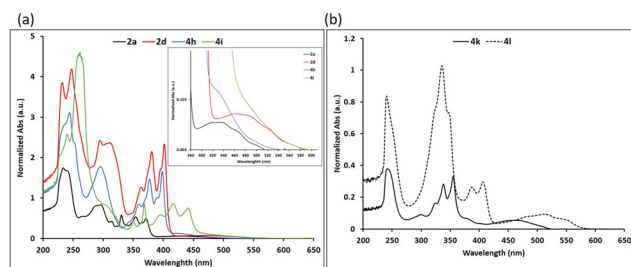
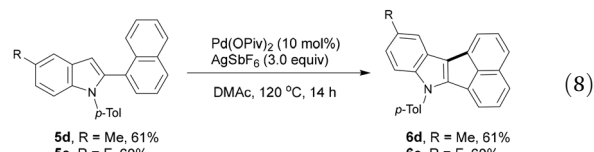
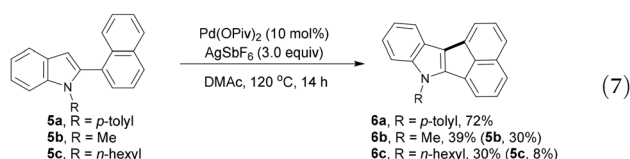


**Fig. 1** UV-Vis absorption spectra in CHCl<sub>3</sub>, (a) **2a**, **2d**, **4h**, and **4i**; (b) **4k** and **4l**.



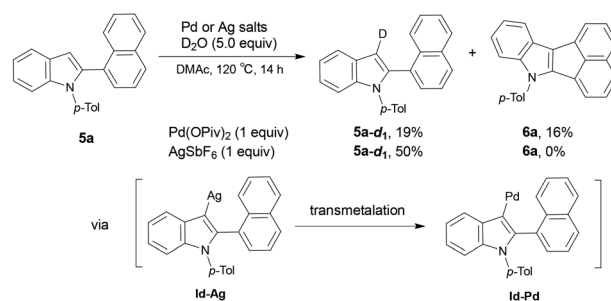
process at the nucleophilic C3 position of **1a**. On the other hand, copper salts such as  $\text{Cu}(\text{OPiv})_2$  and  $\text{Cu}(\text{OTf})_2$  exhibited lower performance compared to silver salts (entries 5 and 6). In comparison, the combination of  $\text{PdCl}_2$  with  $\text{AgSbF}_6$  was found to be ineffective, suggesting that a pivalate counteranion is required to sufficiently implement this C–H/C–H coupling reaction (entry 7).

To compare the site-selective reactivity of the C–H bond at the C3 and C2 positions, the indole substrate **5a'** bearing a 1-naphthyl group at the C3 position was subjected to the  $\text{PdCl}_2/\text{AgSbF}_6$  system (eqn (6)). As expected, the yield of the corresponding product **6a** was very low (14%), indicating that the C3 position of the indole is much more reactive than the C2 position under the present conditions. The *N*-methyl- and *N*-hexyl-substituted indoles **5b** and **5c** were examined to be less effective compared to the *N*-*p*-tolyl-substituted indole **5a**, affording the corresponding products **6b** and **6c** in 39% and 30% yields, respectively (eqn (7)). The decreased yields of **6b** and **6c** could be attributed to the partial decomposition of **5b** and **5c**, likely due to *N*-dealkylation of the methyl or hexyl groups on the indole moiety under Pd-catalysed conditions.<sup>9</sup> In contrast, the *N*-*p*-tolyl group of **5a** was highly tolerant to *N*-dearylation, affording **6a** in good yield. It should be noted that we have previously developed an efficient Pd-catalyzed cascade cyclization for the synthesis of *N*-alkyl-substituted CP-PHAs such as **6c**, as shown in Scheme 1c.<sup>9</sup> Therefore, the present direct C–H/C–H coupling of *N*-aryl-substituted indoles can be considered as an alternative method for the synthesis of these indole-fused CP-PHAs. It was noted that the *N*-unsubstituted indole substrate was almost completely ineffective in yielding the corresponding CP-PHA product. In addition, indoles **5d** and **5e** bearing an electron-donating methyl group and an electron-withdrawing fluorine group at the 5-position (R) of the indole moiety, respectively, showed no obvious electronic effect in the formation of the corresponding products **6d** and **6e** in good yields (eqn (8)). Our previous electrochemical studies revealed that the HOMO and LUMO of such indole-fused CP-PHA analogues containing naphthalene, pyrene, and phenanthrene are in the range of  $-5.25$  to  $-5.12$  eV and  $-3.37$  to  $-2.97$  eV, respectively,<sup>9</sup> which are higher than those of the (benzo)thiophene analogues as shown in Table 3 due to the stronger electron-donating nature of the indole moiety compared to the (benzo)thiophene moieties.

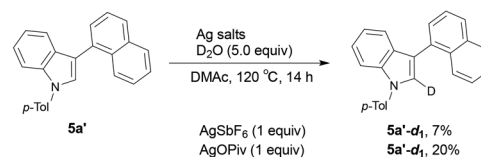


To confirm the involvement of the C–H metalation process, we performed the H/D exchange reaction using **5a** and  $\text{D}_2\text{O}$ . The reaction with 1 equiv. of  $\text{Pd}(\text{OPiv})_2$  without using  $\text{AgSbF}_6$  afforded the deuterated product **5a-d<sub>1</sub>** in 19% yield together with the corresponding coupling product **6a** in 16% yield (Scheme 5a). This result indicates that  $\text{Pd}(\text{OPiv})_2$  is able to promote C–H metalation at the C3 position of **5a** via the formation of an indole-Pd (**Id-Pd**) intermediate, followed by activation of the *peri*-C–H bond to give **6a**. Meanwhile, the use of 1 equiv. of  $\text{AgSbF}_6$  afforded **5a** in 50% yield without producing **6a**, indicating that the C–H metalation reactivity of  $\text{AgSbF}_6$  at the C3 position of **5a** is higher than that of  $\text{Pd}(\text{OPiv})_2$ , leading to the formation of the an indole-Ag (**Id-Ag**) intermediate. The fact that the combination of  $\text{Pd}(\text{OPiv})_2$  catalyst with  $\text{AgSbF}_6$  significantly improved the yield of **6a** supports the involvement of the **Id-Ag** to **Id-Pd** transmetalation in the present C–H/C–H coupling reaction. Additionally, no deuterium incorporation was observed at the 2- or 8-positions of the naphthyl moiety of **5a**, **5a-d<sub>1</sub>**, and **6a** after these deuterium reactions. Furthermore, H/D exchange experiments with **5a'** bearing a 1-naphthyl group at the C3 position in the presence of 1 equiv. of  $\text{AgSbF}_6$  or  $\text{AgOPiv}$ , respectively, afforded the corresponding deuteration product **5a'-d<sub>1</sub>** in low yields (Scheme 5b). These results are in line with the hypothesized difference in nucleophilicity between the C2 and C3 positions of indole as well as the difference in C–H bond acidity between benzothiophene and indole.

(a) Deuteration of the C3 position of **5a**

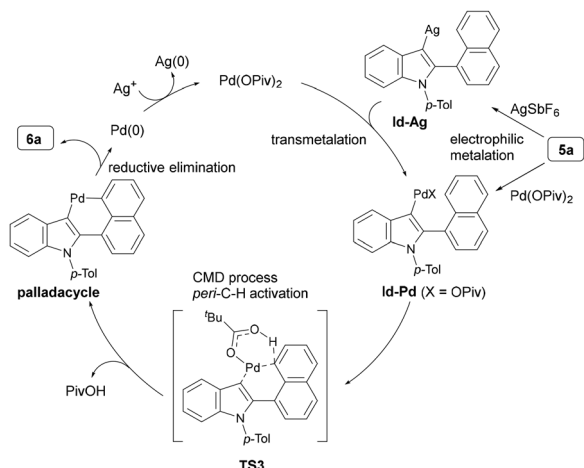


(b) Deuteration of the C2 position of **5a'**



**Scheme 5** Study for the role of Ag and Pd salts.  $^1\text{H}$  NMR yields are shown using  $\text{CH}_2\text{Br}_2$  as an internal standard.





**Scheme 6** Plausible reaction mechanism for the formation of **6a**.

Based on the experimental outcomes, a plausible reaction mechanism for the direct indole-C-H/*peri*-C-H coupling was proposed as shown in Scheme 6. Electrophilic metalation at the C3 position of **5a**, involving electrophilic substitution of both  $\text{AgSbF}_6$  and  $\text{Pd}(\text{OPiv})_2$  and followed by deprotonation, leads to the formation of intermediates **Id-Ag** and **In-Pd**, respectively, with the former predominating. The **Id-Ag** intermediate then undergoes transmetalation with  $\text{Pd}(\text{OPiv})_2$  to form **Id-Pd**, which activates the *peri*-C-H bond *via* a CMD process with a pivalate counteranion-assisted transition state (**TS3**) to generate a palladacycle intermediate. Reductive elimination of the palladacycle furnishes the coupling product **6a**. Finally, the reduced  $\text{Pd}(0)$  species is oxidized by a silver oxidant to regenerate the active  $\text{Pd}(\text{II})$  species.

## Conclusions

We have disclosed for the first time a new and efficient Pd-catalyzed direct aromatic C-H/*peri*-C-H coupling reaction *via* site-specific C-H bond activation of heteroaromatics, such as benzo[*b*]thiophenes, thiophenes, and indoles, as well as *peri*-C-H bond activation of various PAHs to construct diverse CP-fused PHAs. The choice of silver salts with respect to the reactive site of the heteroaromatics is found to be crucial for the implementation of this Pd-catalyzed site-specific coupling reaction:  $\text{AgOPiv}$  with pivalate counteranion enables C-H metalation at the C2 position of benzo[*b*]thiophenes and thiophenes, whereas the cationic  $\text{AgSbF}_6$  favors C-H metalation at the C3 position of indoles. The present dual C-H functionalization does not require any directing groups or prehalogenation of the *peri*-position of polyaromatic unit and the heteroaromatic unit, providing an alternative, convenient, and straightforward approach to construct new CP-PHAs fused with various large PAHs and  $\pi$ -extended CP-PHAs fused with two CP rings, which are difficult to achieve by the reported synthetic methods. Further extension of the current dual C-H annulation strategy to the design and synthesis of novel

$\pi$ -extended PHAs fused with various ring systems is in progress to discover new organic functional materials.

## Author contributions

T. J. and M. T. conceived the methodology and wrote the manuscript. M. K. and S. A. performed experiments, measurements, and theoretical calculations. All the authors analysed the data.

## Data availability

Experimental procedures, computational data, and characterization of related compounds are provided in the ESI.†

## Conflicts of interest

There are no conflicts to declare.

## Acknowledgements

This research was supported by a Grant-in-Aid for Scientific Research on Innovative Areas "Hybrid Catalysis for Enabling Molecular Synthesis on Demand" (JP17H06447) from MEXT (Japan) and a Grant-in-Aid for Scientific Research (S) (JP22H04969) from the JSPS.

## References

- 1 For review on CP-PAHs, see: Y. T. Wu and J. S. Siegel, Aromatic Molecular-Bowl Hydrocarbons: Synthetic Derivatives, Their Structures, and Physical Properties, *Chem. Rev.*, 2006, **106**, 4843–4867.
- 2 For selected reviews on fullerenes, see: (a) N. Martín, New challenges in fullerene chemistry, *Chem. Commun.*, 2006, 2093–2104; (b) C.-Z. Li, H.-L. Yip and A. K.-Y. Jen, Functional fullerenes for organic photovoltaics, *J. Mater. Chem.*, 2012, **22**, 4161–4177.
- 3 For selected examples on CP-PAHs, see: (a) F. G. Brunetti, X. Gong, M. Tong, A. J. Heeger and F. Wudl, Strain and Hückel Aromaticity: Driving Forces for a Promising New Generation of Electron Acceptors in Organic Electronics, *Angew. Chem., Int. Ed.*, 2010, **49**, 532–536; (b) D. T. Chase, A. G. Fix, B. D. Rose, C. D. Weber, S. Nobusue, C. E. Stockwell, L. N. Zakharov, M. C. Lonergan and M. M. Haley, Electron-Accepting 6,12-Diethynylindeno[1,2-*b*]fluorenes: Synthesis, Crystal Structures, and Photophysical Properties, *Angew. Chem., Int. Ed.*, 2011, **50**, 11103–11106; (c) C. H. Lee and K. N. Plunkett, Orthogonal Functionalization of Cyclopenta[*hi*]aceanthrylenes, *Org. Lett.*, 2013, **15**, 1202–1205; (d) D. T. Chase, A. G. Fix, S. J. Kang, B. D. Rose, C. D. Weber, Y. Zhong,



- L. N. Zakharov, M. C. Lonergan, C. Nuckolls and M. M. Haley, 6,12-Diarylindeno[1,2-*b*]fluorenes: Syntheses, Photophysics, and Ambipolar OFETs, *J. Am. Chem. Soc.*, 2012, **134**, 10349–10352; (e) J. D. Wood, J. L. Jellison, A. D. Finke, L. Wang and K. N. Plunkett, Electron Acceptors Based on Functionalizable Cyclopenta[*hi*]aceanthrylenes and Dicyclopenta[*de,mn*]tetracenes, *J. Am. Chem. Soc.*, 2012, **134**, 15783–15789; (f) H. Xia, D. Liu, X. Xu and Q. Miao, Ambipolar organic semiconductors from electron-accepting cyclopenta-fused anthracene, *Chem. Commun.*, 2013, **49**, 4301–4303; (g) R. Q. Lu, Y. Q. Zheng, Y. N. Zhou, X. Y. Yan, T. Lei, K. Shi, Y. Zhou, J. Pei, L. Zoppi, K. K. Baldrige, J. S. Siegel and X. Y. Cao, Corannulene derivatives as non-fullerene acceptors in solution-processed bulk heterojunction solar cells, *J. Mater. Chem. A*, 2014, **2**, 20515–20519; (h) A. N. Lakshminarayana, J. Chang, J. Luo, B. Zheng, K.-W. Huang and C. Chi, Bisindeno-annulated pentacenes with exceptionally high photo-stability and ordered molecular packing: simple synthesis by a regioselective Scholl reaction, *Chem. Commun.*, 2015, **51**, 3604–3607; (i) L. J. Purvis, X. Gu, S. Ghosh, Z. Zhang and C. J. Cramer, Douglas, Synthesis and Characterization of Electron-Deficient Asymmetrically Substituted Diarylindenetetracenes, *J. Org. Chem.*, 2018, **83**, 1828–1841; (j) Q. Xu, C. Wang, Y. Zhao, D. Zheng, C. Shao, W. Guo, X. Deng, Y. Wang, X. Chen, J. Zhu and H. Jiang, Tuning the Properties of Corannulene-Based Polycyclic Aromatic Hydrocarbons by Varying the Fusing Positions of Corannulene, *Org. Lett.*, 2020, **22**, 7397–7402; (k) Y. Tanaka, N. Fukui and H. Shinokubo, as-Indaceno[3,2,1,8,7,6-*ghijklm*]terylene as a near-infrared absorbing C70-fragment, *Nat. Commun.*, 2020, **11**, 3873.
- 4 For reviews on PHAs, see: (a) M. Stepień, E. Gońka, M. Żyła and N. Sprutta, Heterocyclic Nanographenes and Other Polycyclic Heteroaromatic Compounds: Synthetic Routes, Properties, and Applications, *Chem. Rev.*, 2017, **117**, 3479–3716; (b) A. Borissov, Y. K. Maurya, L. Moshniaha, W.-S. Wong, M.-K. Żyła-Karwowska and M. Stepień, Recent Advances in Heterocyclic Nanographenes and Other Polycyclic Heteroaromatic Compounds, *Chem. Rev.*, 2022, **122**, 565–788.
- 5 For selected examples on CP-PHAs, see: (a) Y. Matano, A. Saito, T. Fukushima, Y. Tokudome, F. Suzuki, D. Sakamaki, H. Kaji, A. Ito, K. Tanaka and H. Imahori, Fusion of Phosphole and 1,1'-Biacenaphthene: Phosphorus (v)-Containing Extended  $\pi$ -Systems with High Electron Affinity and Electron Mobility, *Angew. Chem., Int. Ed.*, 2011, **50**, 8016–8020; (b) A. R. Mohebbi, J. Yuen, J. Fan, C. Munoz, M. F. Wang, R. S. Shirazi, J. Seifter and F. Wudl, Emeraldicene as an Acceptor Moiety: Balanced-Mobility, Ambipolar, Organic Thin-Film Transistors, *Adv. Mater.*, 2011, **23**, 4644–4648; (c) A. R. Mohebbi and F. Wudl, Electron-Accepting Dithiarubicene (Emeraldicene) and Derivatives Prepared by Unprecedented Nucleophilic Hydrogen Substitution by Alkylolithium Reagents, *Chem. – Eur. J.*, 2011, **17**, 2642–2646; (d) Y. Nagasaka, C. Kitamura, H. Kurata and T. Kawase, Diacenaphtho[1,2-*b*;1',2'-*d*]silole and -pyrrole, *Chem. Lett.*, 2011, **40**, 1437–1439; (e) M. Mahmut, T. Awut, I. Nurulla and M. Mijit, Synthesis of two novel acenaphthyl-quinoxaline based low-band gap polymers and its electrochromic properties, *J. Polym. Res.*, 2014, **21**, 1–9; (f) K. Tsukamoto, K. Takagi, S. Nagano, M. Hara, Y. Le, K. Osakada and D. Takeuchi,  $\pi$ -Extension of electron-accepting dithiarubicene with a cyano-substituted electron-withdrawing group and application in air-stable n-channel organic field effect transistors, *J. Mater. Chem. C*, 2019, **7**, 12610–12618; (g) W. A. Hussain and K. N. Plunkett, Benzodithiophene-Fused Cyclopentannulated Aromatics via a Palladium-Catalyzed Cyclopentannulation and Scholl Cyclodehydrogenation Strategy, *J. Org. Chem.*, 2021, **86**, 12569–12576.
- 6 For review on *peri*-C-H annulation, see: T. Jin, Z. Zhao, N. Asao and Y. Yamamoto, Metal-Catalyzed Annulation Reactions for  $\pi$ -Conjugated Polycycles, *Chem. – Eur. J.*, 2014, **20**, 3554–3576.
- 7 (a) H. A. Wegner, L. T. Scott and A. de Meijere, A New Suzuki-Heck-Type Coupling Cascade: Indeno[1,2,3]-Annulation of Polycyclic Aromatic Hydrocarbons, *J. Org. Chem.*, 2003, **68**, 883–887; (b) H. A. Wegner, H. Reisch, K. Rauch, A. Demeter, K. A. Zachariasse, A. de Meijere and L. T. Scott, Oligoindenopyrenes: A New Class of Polycyclic Aromatics, *J. Org. Chem.*, 2006, **71**, 9080–9087.
- 8 H. Wu, R. Fang, J. Tao, D. Wang, X. Qiao, X. Yang, F. Hartl and H. Li, Diacenaphthylene-fused benzo[1,2-*b*:4,5-*b'*]dithiophenes: polycyclic heteroacenes containing full-carbon five-membered aromatic rings, *Chem. Commun.*, 2017, **53**, 751–754.
- 9 T. Jin, S. Suzuki, H. E. Ho, H. Matsuyama, M. Kawata and M. Terada, Pd-Catalyzed Indolization/*peri*-C–H Annulation/N-Dealkylation Cascade to Cyclopenta-Fused Acenaphtho [1,2-*b*]indole Scaffold, *Org. Lett.*, 2021, **23**, 9431–9435.
- 10 (a) B. Yao, Q. Wang and J. Zhu, Palladium-Catalyzed Coupling of *ortho*-Alkynylanilines with Terminal Alkynes Under Aerobic Conditions: Efficient Synthesis of 2,3-Disubstituted 3-Alkynylindoles, *Angew. Chem., Int. Ed.*, 2012, **51**, 12311–12315; (b) B. Yao, Q. Wang and J. Zhu, Palladium(II)-Catalyzed Intramolecular Diamination of Alkynes under Aerobic Oxidative Conditions: Catalytic Turnover of an Iodide Ion, *Angew. Chem., Int. Ed.*, 2012, **51**, 5170–5174; (c) X.-F. Xia, N. Wang, L.-L. Zhang, X.-R. Song, X.-Y. Liu and Y.-M. Liang, Palladium(II)-Catalyzed Tandem Cyclization/C–H Functionalization of Alkynes for the Synthesis of Functionalized Indoles, *J. Org. Chem.*, 2012, **77**, 9163–9170; (d) B. Yao, Q. Wang and J. Zhu, Palladium (II)-Catalyzed Cyclizative Cross-Coupling of *ortho*-Alkynylanilines with *ortho*-Alkynylbenzamides under Aerobic Conditions, *Angew. Chem., Int. Ed.*, 2013, **52**, 12992–12996; (e) S. Zhang, H. Ma, H. E. Ho, Y. Yamamoto, M. Bao and T. Jin, Pd-Catalyzed cascade cyclization of *o*-alkynylanilines via C–H/C–N bond cleavage leading to dibenzo[*a,c*]carbazoles, *Org. Biomol. Chem.*, 2018, **16**, 5236–5240.





- 11 For selected examples on transition-metal-catalyzed *peri*-C–H annulation, see: (a) H. Dang and M. A. Garcia-Garibay, Palladium-Catalyzed Formation of Aceanthrylenes: A Simple Method for Peri-Cyclopentenelation of Aromatic Compounds, *J. Am. Chem. Soc.*, 2001, **123**, 355–356; (b) S. Mochida, M. Shimizu, K. Hirano, T. Satoh and M. Miura, Synthesis of Naphtho[1,8-*bc*]pyran Derivatives and Related Compounds through Hydroxy Group Directed C–H Bond Cleavage under Rhodium Catalysis, *Chem. – Asian J.*, 2010, **5**, 847–851; (c) V. S. Thirunavukkarasu, M. Donati and L. Ackermann, Hydroxyl-Directed Ruthenium-Catalyzed C–H Bond Functionalization: Versatile Access to Fluorescent Pyrans, *Org. Lett.*, 2012, **14**, 3416–3419; (d) X. Zhang, W. Si, M. Bao, N. Asao, Y. Yamamoto and T. Jin, Rh(III)-Catalyzed Regioselective Functionalization of C–H Bonds of Naphthylcarbamates for Oxidative Annulation with Alkyne, *Org. Lett.*, 2014, **16**, 4830–4833; (e) J. Yin, M. Tan, D. Wu, R. Jiang, C. Li and J. You, Synthesis of Phenalenyl-Fused Pyrylium Cations: Divergent C–H Activation/Annulation Reaction Sequence of Naphthalene Aldehydes with Alkynes, *Angew. Chem., Int. Ed.*, 2017, **56**, 13094–13098; (f) M. Shankar, R. K. Rit, S. Sau, K. Mukherjee, V. Gandon and A. K. Sahoo, Double annulation of *ortho*- and *peri*-C–H bonds of fused (hetero)arenes to unusual oxepino-pyridines, *Chem. Sci.*, 2020, **11**, 10770–10777.
- 12 For selected reviews on aromatic C–H/C–H coupling, see: (a) Y. Yang, J. Lan and J. You, Oxidative C–H/C–H Coupling Reactions between Two (Hetero)arenes, *Chem. Rev.*, 2017, **117**, 8787–8863; (b) I. A. Stepek and K. Itami, Recent Advances in C–H Activation for the Synthesis of  $\pi$ -Extended Materials, *ACS Mater. Lett.*, 2020, **2**, 951–974.
- 13 For selected examples on (hetero)aromatic C–H/C–H coupling without using directing groups, see: (a) D. R. Stuart and K. Fagnou, The Catalytic Cross-Coupling of Unactivated Arenes, *Science*, 2007, **316**, 1172–1175; (b) D. R. Stuart, E. Villemure and K. Fagnou, Elements of Regiocontrol in Palladium-Catalyzed Oxidative Arene Cross-Coupling, *J. Am. Chem. Soc.*, 2007, **129**, 12072–12073; (c) S. J. Tereniak, D. L. Bruns and S. S. Stahl, Pd-Catalyzed Aerobic Oxidative Coupling of Thiophenes: Synergistic Benefits of Phenanthroline Dione and a Cu Cocatalyst, *J. Am. Chem. Soc.*, 2020, **142**, 20318–20323; (d) T. Doba, L. Ilies, W. Sato, R. Shang and E. Nakamura, Iron catalysed regioselective thienyl C–H/C–H coupling, *Nat. Catal.*, 2021, **4**, 631–638.
- 14 (a) K. Masui, H. Ikegami and A. Mori, Palladium-Catalyzed C–H Homocoupling of Thiophenes: Facile Construction of Bithiophene Structure, *J. Am. Chem. Soc.*, 2004, **126**, 5074–5075; (b) M. D. Lotz, N. M. Camasso, A. J. Canty and M. S. Sanford, Role of Silver Salts in Palladium-Catalyzed Arene and Heteroarene C–H Functionalization Reactions, *Organometallics*, 2017, **36**, 165–171.
- 15 (a) B. Liégault, D. Lee, M. P. Huestis, D. R. Stuart and K. Fagnou, Intramolecular Pd(II)-Catalyzed Oxidative Biaryl Synthesis Under Air: Reaction Development and Scope, *J. Org. Chem.*, 2008, **73**, 5022–5028; (b) K. Saito, P. K. Chikkade, M. Kanai and Y. Kuninobu, Palladium-Catalyzed Construction of Heteroatom-Containing  $\pi$ -Conjugated Systems by Intramolecular Oxidative C–H/C–H Coupling Reaction, *Chem. – Eur. J.*, 2015, **21**, 8365–8368; (c) D.-D. Guo, B. Li, D.-Y. Wang, Y.-R. Gao, S.-H. Guo, G.-F. Pan and Y.-Q. Wang, Synthesis of 6*H*-Benzo[*c*]chromenes via Palladium-Catalyzed Intramolecular Dehydrogenative Coupling of Two Aryl C–H Bonds, *Org. Lett.*, 2017, **19**, 798–801.
- 16 (a) K. Shen, Y. Fu, J.-N. Li, L. Liu and Q.-X. Gu, What are the pKa values of C–H bonds in aromatic heterocyclic compounds in DMSO?, *Tetrahedron*, 2007, **63**, 1568–1576; (b) R. R. Fraster, T. S. Mansour and S. Savar, Acidity measurements in THF. V. Heteroaromatic compounds containing 5-membered rings, *Can. J. Chem.*, 1985, **63**, 3505–3509.
- 17 It was observed that the benzofuran substrates exhibited very low reactivity in the present C–H/C–H coupling. For example, the coupling of 3-(naphthalen-1-yl)benzofuran afforded the corresponding annulation product, ace-naphtho[1,2-*b*]benzofuran, in only 8–10% yield, with the starting substrate recovered in 84% yield under standard Pd-catalysed conditions using AgOPiv or AgSbF<sub>6</sub>. Additionally, no reaction was observed when 2-(naphthalen-1-yl)benzofuran was subjected to the standard conditions.
- 18 C. Colletto, A. Panigrahi, J. Fernández-Casado and I. Larrosa, Ag(I)-C–H Activation Enables Near-Room-Temperature Direct  $\alpha$ -Arylation of Benzo[*b*]thiophenes, *J. Am. Chem. Soc.*, 2018, **140**, 9638–9643.
- 19 L. Ackermann, Carboxylate-Assisted Transition-Metal-Catalyzed C–H Bond Functionalizations: Mechanism and Scope, *Chem. Rev.*, 2011, **111**, 1315–1345.

